# We are IntechOpen,
# the world's leading publisher of
# Open Access books
# Built by scientists, for scientists

## 6,900
Open access books available

## 185,000
International authors and editors

## 200M
Downloads

## 154
Countries delivered to

Our authors are among the

## TOP 1%
most cited scientists

## 12.2%
Contributors from top 500 universities

CLARIVATE ANALYTICS

BOOK
CITATION
INDEX

INDEXED

**WEB OF SCIENCE**™

Selection of our books indexed in the Book Citation Index
in Web of Science™ Core Collection (BKCI)

# Interested in publishing with us?
# Contact book.department@intechopen.com

Numbers displayed above are based on latest data collected.
For more information visit www.intechopen.com

# Fatigue and Fracture Behavior of Forging Die Steels

Ryuichiro Ebara
*Hiroshima Institute of Technology,
Japan*

## 1. Introduction

Forging die failures for automotive components are caused by inadequacy of variables such as die materials, die design, die manufacturing and forging operations [1].

The forging die frequently fails from the corner where stress concentrate. Fig.1 shows a typical failure of hot forging die for a knuckle. From the macroscopic fracture surface observation it looks to be easily judged that a brittle failure initiated from the corner. These fractures are frequently observed on hot forging dies for knuckle, connecting rod, crank shaft and flange yoke for automotive components. However it can be clearly identified by low magnification observation that the most of the brittle fractures initiated from short cracks initiated from the corner due to fatigue and thermal fatigue. Fig. 2 shows the fracture surface of a flange yoke die made in SKT4 steel after 2000 forging operations [2]. It is clear that the brittle crack initiated at 3.5mm from the surface where nonmetallic inclusion MnS located. The stretched zone is most frequently observed at the transition zone from fatigue to impact fracture. In this case a stretched zone with 8 to 10μm width was observed between fatigue and impact fracture surface as shown in Fig. 3 [2]. The reason of this failure was determined to be an insufficient preheating temperature for the hot forging die by use of the relationship among dynamic fracture toughness, temperature and stretched zone width. The stretched zone can also be observed in failed cold forging die [3].It is possible to evaluate the fracture toughness of the failed cold forging die for automotive component by measuring the stretched zone width.
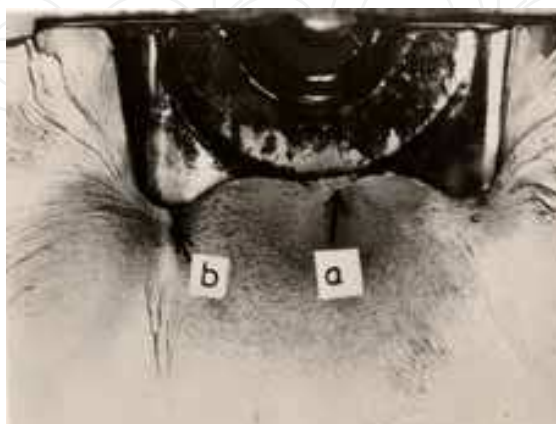


Fig. 1. Macroscopic fracture surface of a knuckle forging die for a motor vehicle [1]. Arrow a and b shows crack initiation area respectively. Forging die steel: SKD62
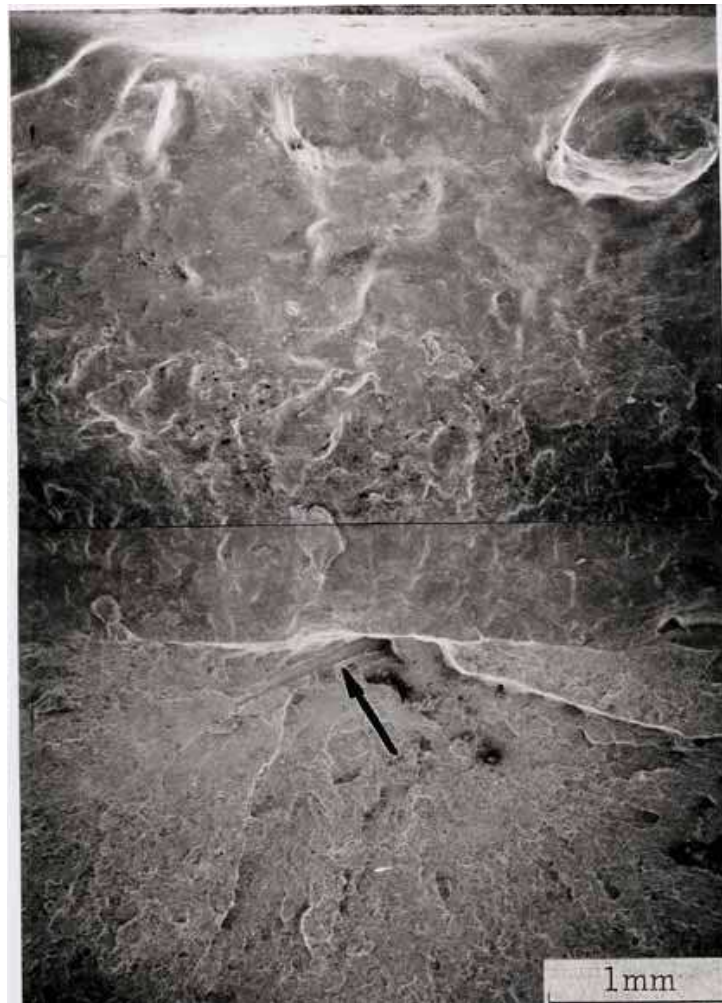
Fig. 2. Fracture surface of a flange york forging die [2]. Arrow shows MnS where impact failure initiated
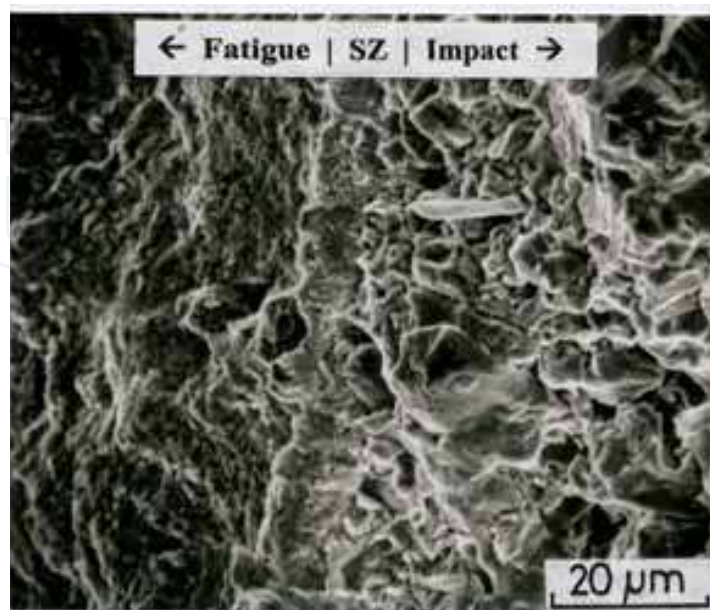


Fig. 3. Stretched zone between fatigue and impact fracture surface [2]. Flange york forging die

Thus it is indispensable to evaluate fatigue and fracture behavior of forging die steels in order to prevent forging die failure and to improve die life. It can also be mentioned that the role of microfractography in failure analysis of forging dies for automotive component is very important.

## 2. Fracture behavior of forging die steels

### 2.1 Hot forging die steels

Instrumented impact tests were conducted for fatigue crack introduced 2 mm U notched Charpy impact specimens. Fig.4 shows dynamic impact fracture toughness $K_{1d}$ as a function of testing temperature for SKD 61 steel. Maximum $K_{1d}$ is attained at 573K. The ductile-brittle transition temperature is observed at around 423K.
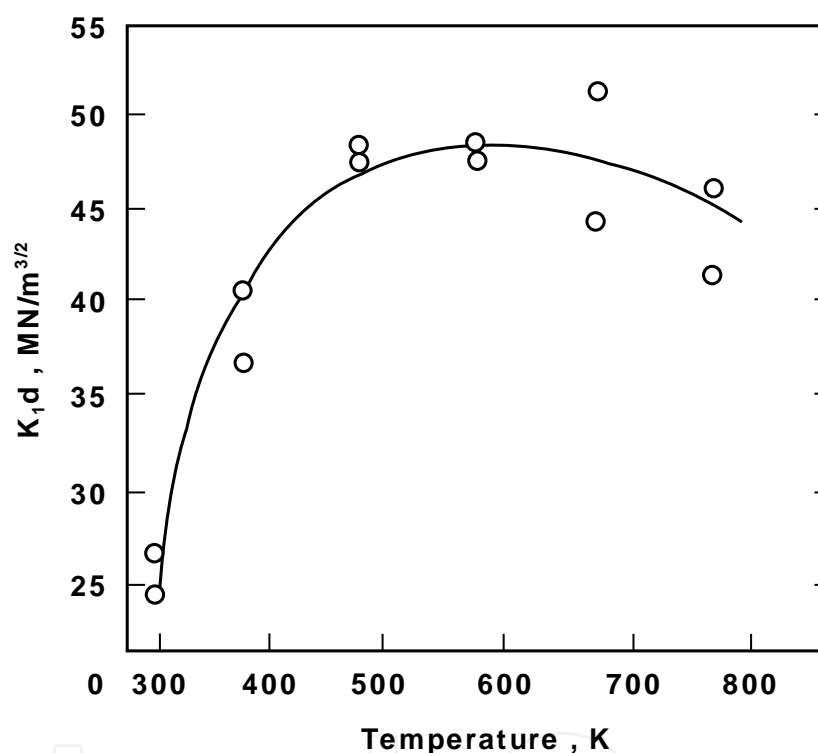


Fig. 4. Dynamic fracture toughness, $K_{1d}$ as a function of tested temperature [4].

Fig. 5 shows impact fracture surfaces of SKD62 steel. Cleavage fracture is observed at room temperature (Fig. 5 a)), while dimple is observed at 673K (Fig. 5 b)). In general ductile-brittle transition temperature is in the range of 373K to 423K for hot forging die steel. Mixed mode of cleavage and intercrystalline fracture is predominant at temperature lower than ductile-brittle transition temperature, while dimple is predominant at temperature higher than ductile-brittle transition temperature. Thus impact fracture whether ductile or brittle can be qualitatively identified by use of microfractography of these impact fracture surface characteristics. Fig. 6 shows stretched zone observed between fatigue and impact fracture surface of hot forging die steel SKD62.The higher the testing temperature the wider the stretched zone width is. Fig. 7 shows $K_{1d}$ as a function of stretched zone width. As afore mentioned the failed temperature of hot forging die failure can be quantitatively determined by measuring stretched zone width on fracture surface.
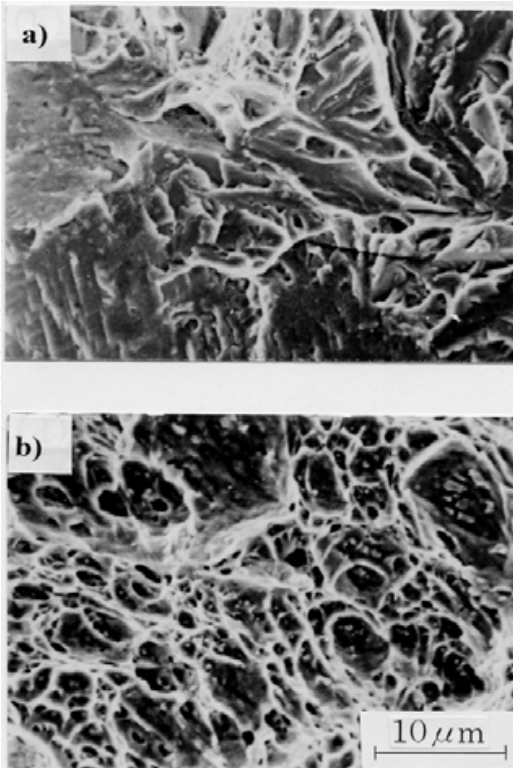
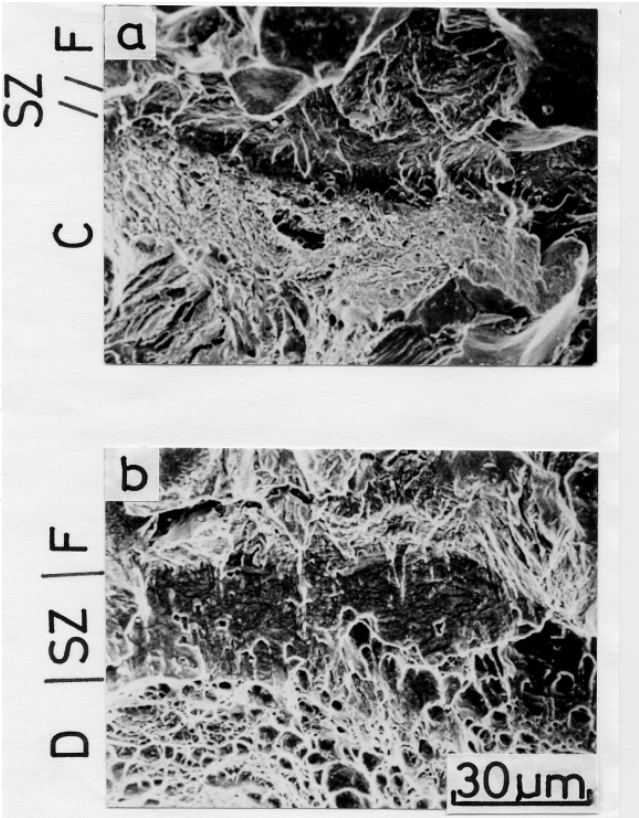Fig. 5. Impact fracture surface, SKD62[4]. a) RT b) 673K



Fig. 6. Stretched zone, SKD62[4]. a) RT b) 673K, SZ: stretched zone, F: fatigue, C: cleavage , D: dimple
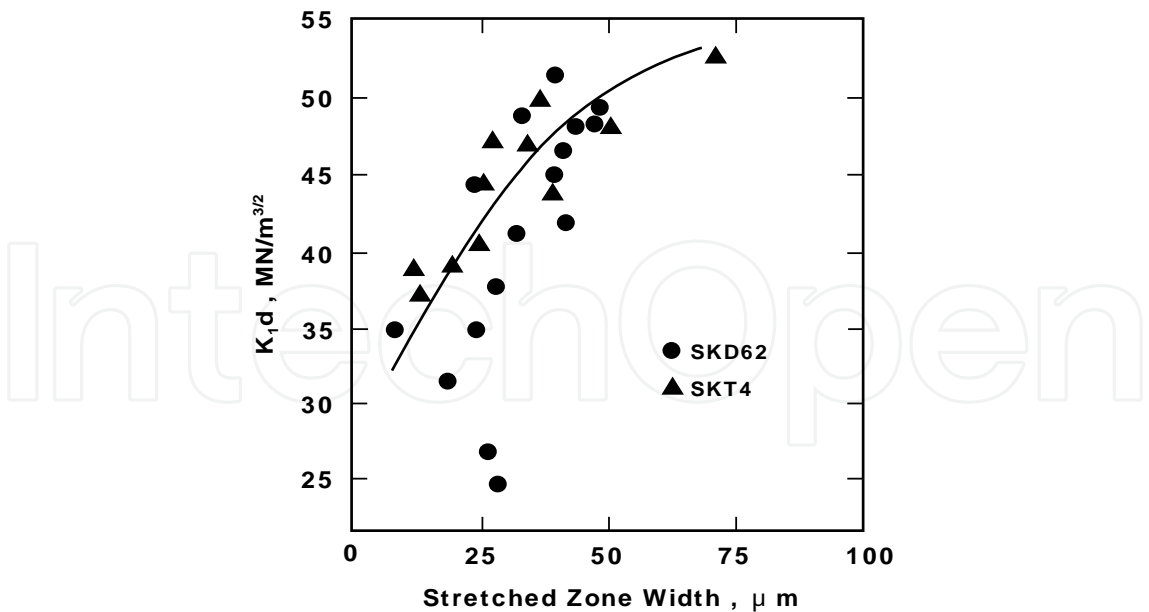
Fig. 7. Dynamic fracture toughness $K_{1d}$ as a function of stretched zone width[4].

## 2.2 Cold forging die steels

Fig. 8 shows the Charpy Impact test results investigated for specimens with 5mm U notch, 2.5 mm saw cut and 2.5mm saw cut with fatigue crack (1.64-2.25mm)[3]. The commercial cold forging die steels such as tool steels of SKD61, SKD11 and QCM8, high speed steels of YXM1,YXM4,YXR3,YXR33 and YXR3,powdered high speed steel of HAP72 and cemented carbide GM60 were used. These steels were quenched and tempered and the Rockwell C scale hardness numbers are 52 to 67 [5].
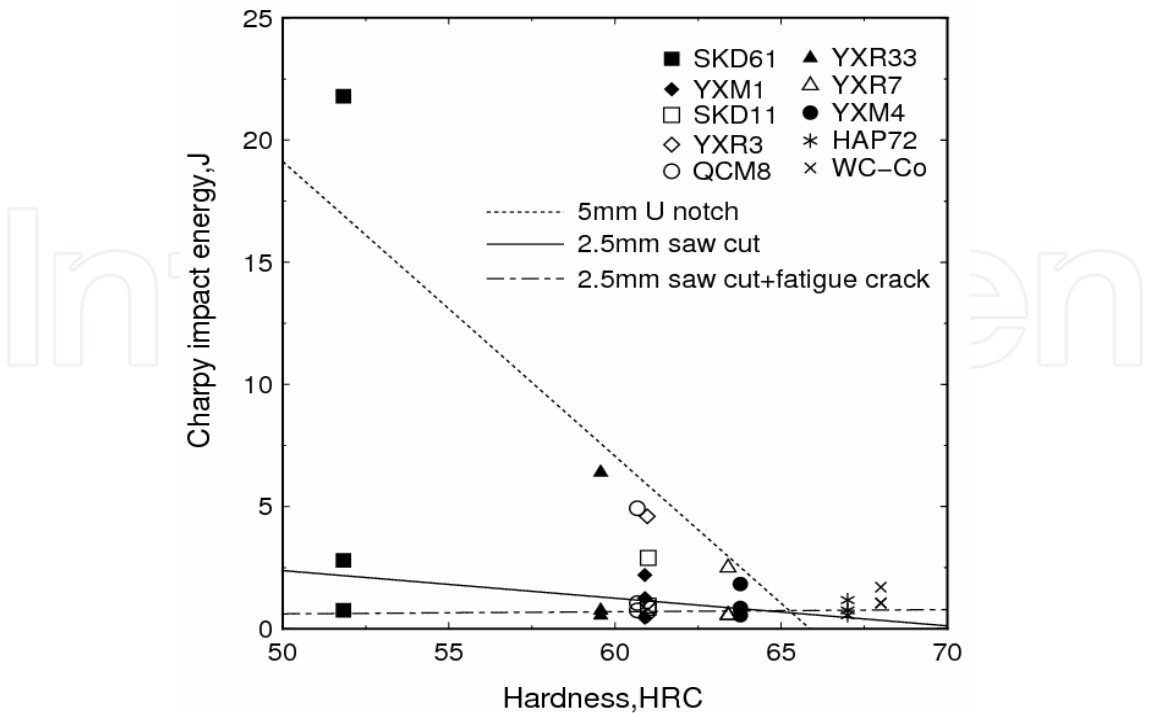


Fig. 8. Charpy impact energy of cold forging die steels with different notch figure [3].

The Charpy impact energy of cold forging die steels is very sensitive to the notch figure. The most prominent notch effect can be observed in SKD61. The larger the hardness the smaller the Charpy impact energy is. The Charpy impact energy of cold forging die steels was low as compared with those of other ductile structural steels. Macroscopic fracture surfaces of 5mm U notched specimens were brittle with radial zone. The shear lips were observed on SKD61 with relatively smaller hardness. Macroscopic fracture surfaces of 2.5mm saw cut and 2.5mm saw cut with fatigue crack were more brittle.
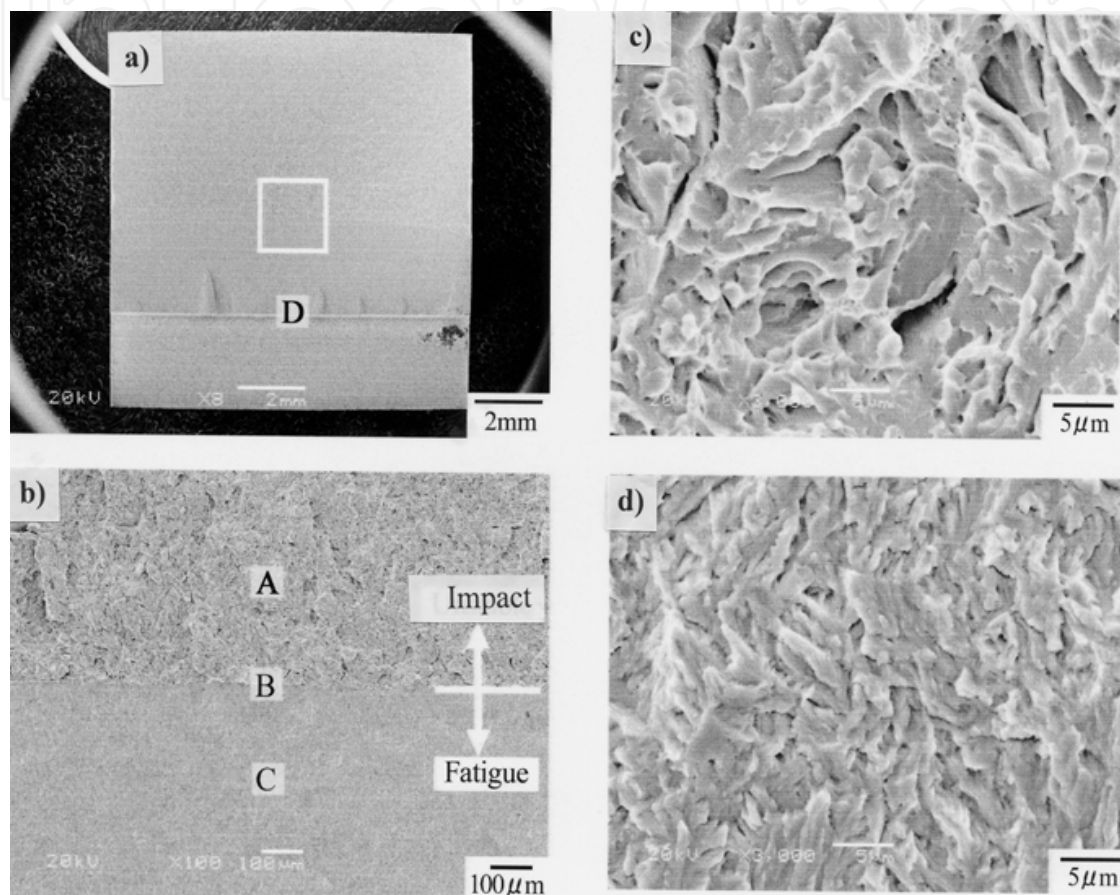


Fig. 9. Impact fracture surface. SKD61, HRC 52, 2.5mm saw cut with fatigue crack[3]. a) Macroscopic fracture surface, b) Enlargement of the window area in a), c) Impact fracture surface (A in c)), Fatigue fracture surface(C in c))

Cleavage fracture surfaces are predominantly observed on fracture surfaces of all tested steels except WC-Co. The fracture surface of WC-Co was intergranular. Fig. 9 shows fracture surface of 2.5mm saw cut with fatigue crack in SKD61. It can be easily discriminate fatigue fracture surface from impact fracture surface even in macroscopic fracture surface (Fig. 9a)). The discrimination is much more easily in low magnified fracture surface for the window area in Fig. 9a) (Fig. 9b)). The discrimination is not easy for the steel such as HAP72 with higher hardness of HTC67.The fatigue fracture surface was transgranular (Fig. 9d)) and impact fracture surface was cleavage (Fig. 9c)) for tool steels and high speed steels. However intergranular fracture is predominant for WC-Co. The stretched zone was clearly observed between fatigue fracture surface and impact fracture surface for tool steels and high speed steels. The stretched zone width is wider in the steel with lower hardness. For hard steels

the stretched zone can be identified for powdered steel HAP72 (Fig. 11d)), while it can not be easily identified for sintered steel WC-Co.

The three point bending fracture toughness tests were conducted in accordance with ASTM Standard E399-90 by use of the specimen with 55mm long, 10mm wide and 10mm thick. Fatigue crack with length of 1.64 to 2.25mm was introduced ahead of saw cut notch with 2.5 mm long[3]. Fig.10 shows the relation between fracture toughness and hardness of cold forging die steels. The higher the hardness the lower the fracture toughness was. The relation between hardness and fracture toughness can be expressed as follows.

$$\text{Fracture toughness (MPa}\sqrt{m}\text{ )} = -1.445 \times \text{HRC} + 110.37$$

Fracture surface morphology of three point bending fracture surfaces are basically same as that of the Charpy impact fracture surfaces with 2.5mm saw cut with fatigue crack. The morphology of the fatigue and unstable fracture surface of the three point bending fracture surface was same as that of the impact fracture. The stretched zone is clearly observed on fracture surface between fatigue and unstable fracture.
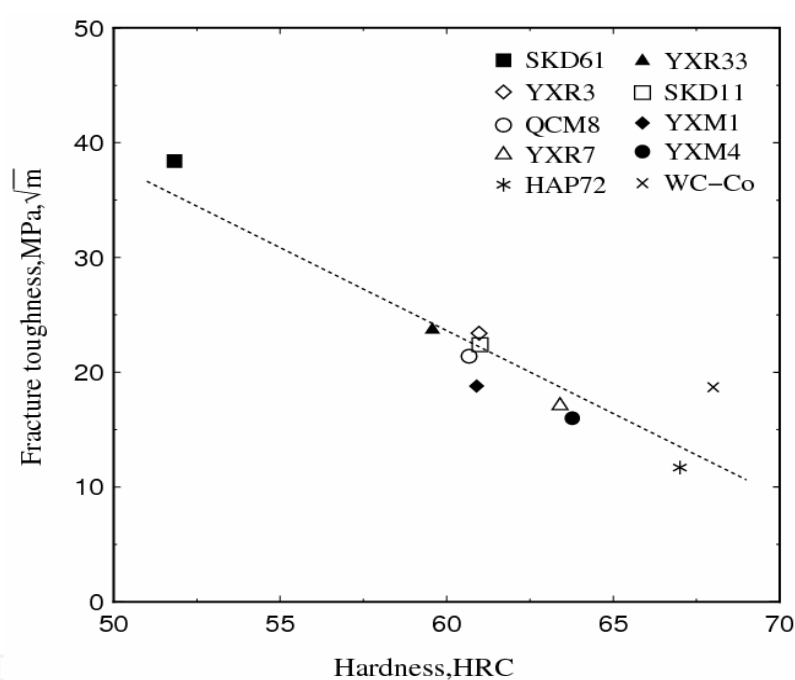


Fig. 10. Relation between fracture toughness and hardness of cold forging die steels[3].

Fig. 11. shows three point bending fracture surfaces of SKD62 and HAP72. It is easily discriminate between fatigue and unstable fracture surface from macroscopic fracture surfaces [Fig. 11a), c)]. The stretched zone can be clearly identified between fatigue and unstable fracture surface [Fig.11b), d)]. It was reported by Bates and Clark that the stretched zone width can be well correlated to fracture toughness [7]. The $Kc/\sigma_y$ can be depicted for various kinds of structural materials including cold forging die steels as shown in Fig. 12. The relation between SZW (µm) and $Kc/\sigma_y(\sqrt{mm})$ can be expressed as shown below.

$$\text{SZW(µm)} = 3.28(Kc/\sigma_y)^{1.24}$$

This relation shows that the quantitative analysis is possible by measuring the stretched zone width on fracture surface in the failure analysis of cold forging dies.
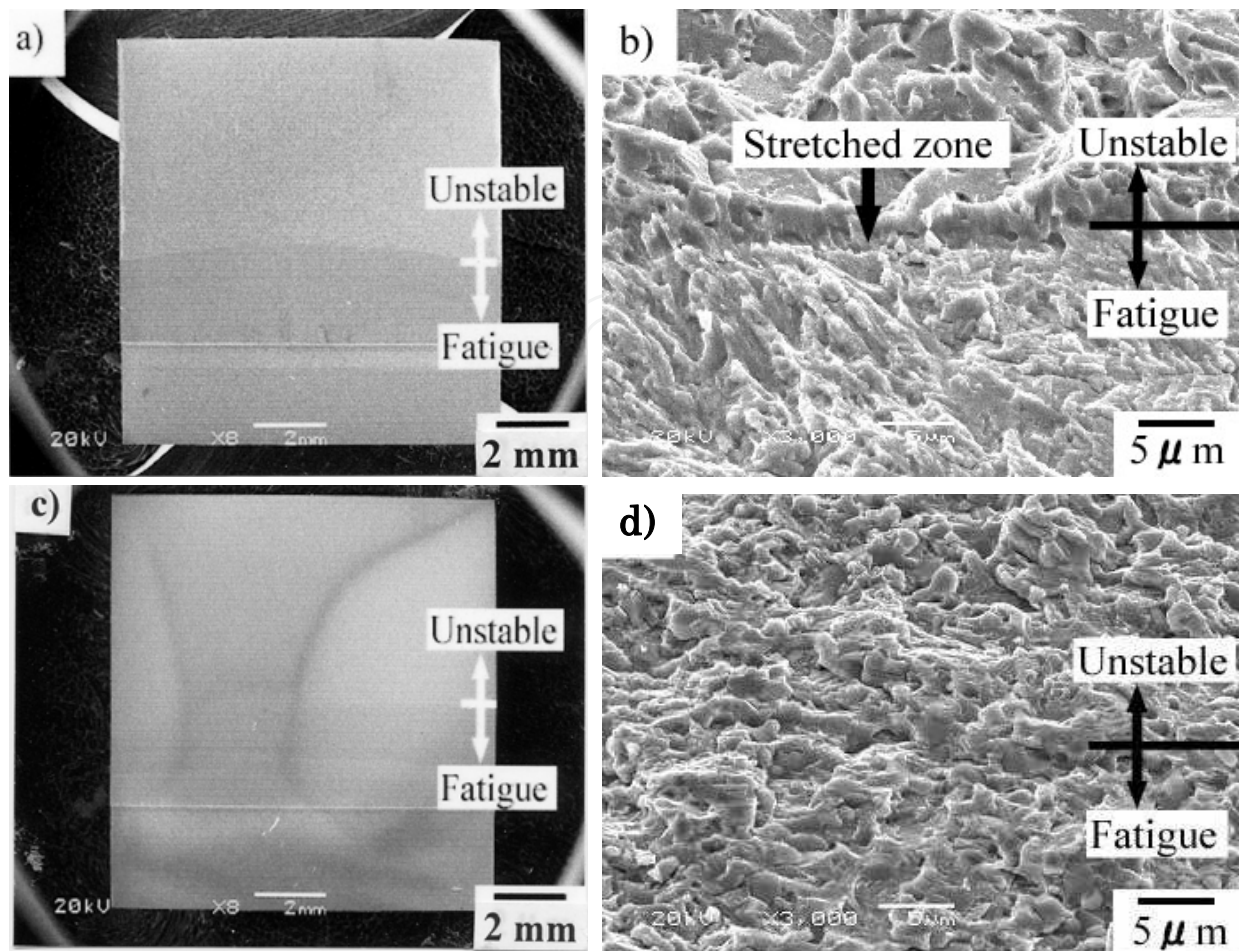
Fig. 11. Stretched zone on three point bending fracture surface[3]. a), b) SKD61 c), d) HAP72

## 3. Fatigue behavior of forging die steels

### 3.1 Hot forging die steels

Effect of testing temperature, steel hardness, stress concentration factor of specimen and surface treatments effect on low cycle fatigue strength of hot forging die steels are mainly evaluated. Load controlled low cycle fatigue tests were conducted at 473K and 673K by use of an axial fatigue testing machine (98kN). Round notched bar specimen with minimum diameter of 8mm was used. The stress concentration factor was 1.31. Testing frequency was 0.083Hz and R value (minimum to maximum stress in the loading cycle) was 0.05.

Fig. 13 shows low cycle fatigue strength of hot forging die steels with different hardness under various temperatures. The low cycle fatigue strength at RT was almost same as that at 473K and 14% higher than that at 723K. It was also obtained that the low cycle fatigue strength of the notched specimen with stress concentration factor of 2.3 for SKD62 with HRC43.5 at 573K was almost same as that at RT as shown in Fig. 14. [4]. Therefore it can be mentioned that temperature effect on the low cycle fatigue strength of SKD62 appears in a temperature range over than 573K. The fatigue strength of SKD62 with HRC46 at $10^4$ cycles was 25, 10 and 13% higher than that of SKD62 with HRC43.5 at tested temperatures of RT, 573K and 723K. The major reason for the fatigue strength increase in SKD62 with higher hardness is attributed to the delay of fatigue crack initiation due to the higher ultimate tensile strength.
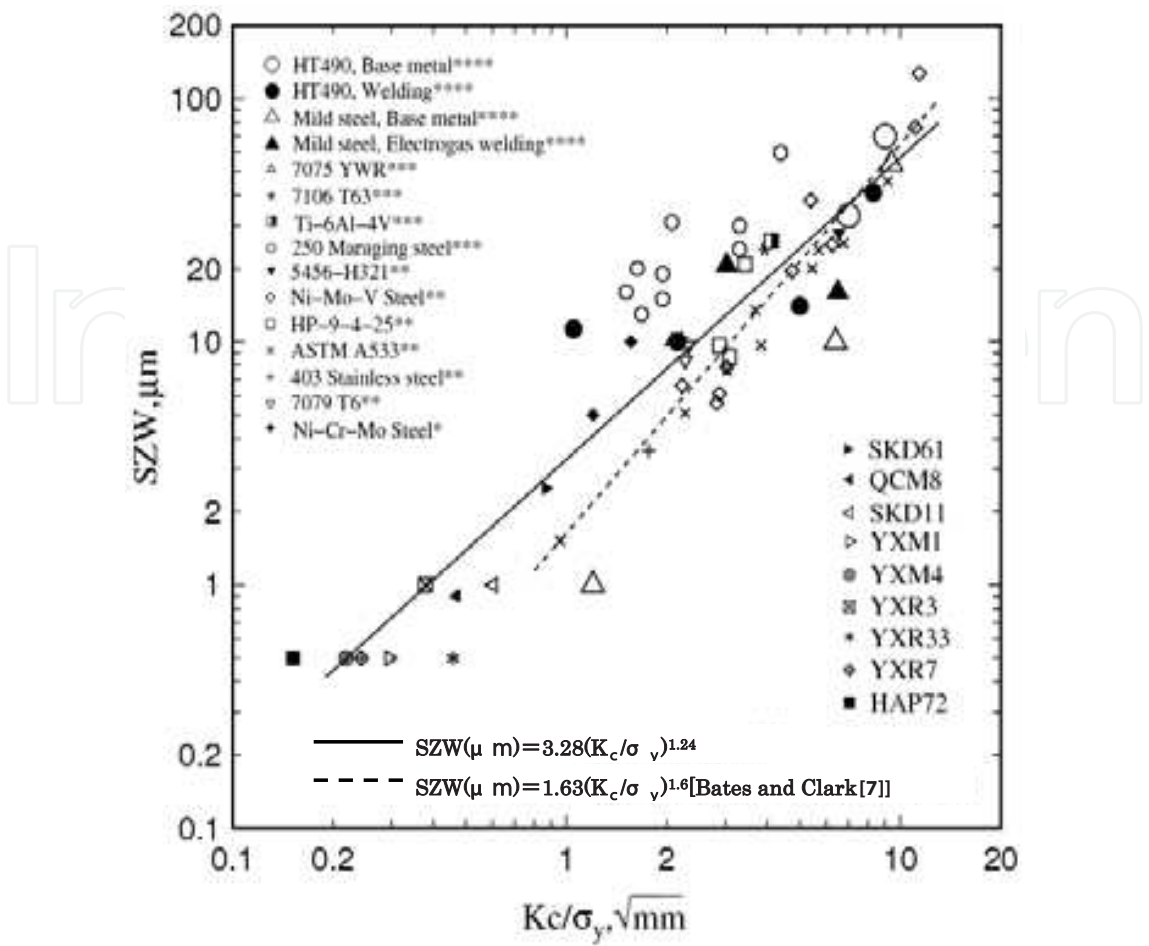
Fig. 12. Stretched zone width as a function of Kc/σ$_y$ [3]. *Spitzig[6], **BatesandClark [7], ***Brothers [8], ****Ebara et al. [9]
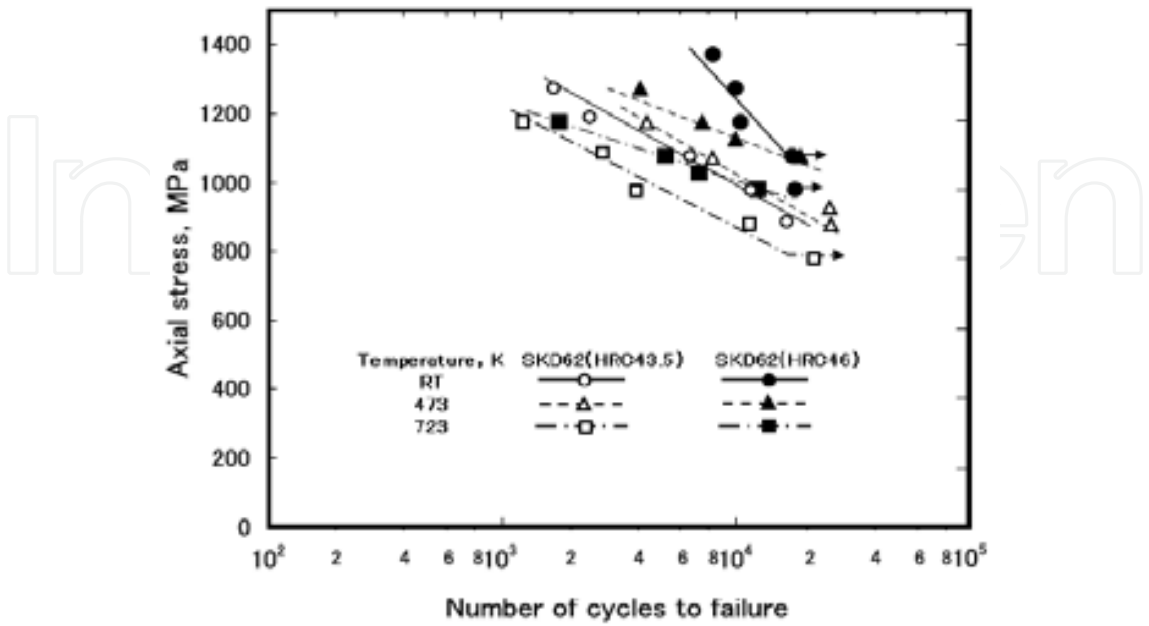


Fig. 13. S-N diagrams of SKD62(HRC43.5) and SKD62(HRC46)[10].

Fig. 14 shows conventional S-N diagrams of base metal, ion nitrided (773Kx30hr) specimen, ion nitrided (723Kx30hr)specimen and tufftrided(843Kx12hr)specimen for SKD62 [4]. The effect of surface treatment such as tufftride and ion nitride cannot be expected at high stress amplitude. Repeated axial stress and number of cycles expected for fatigue strength improvement are summarized in Table 1 [4].
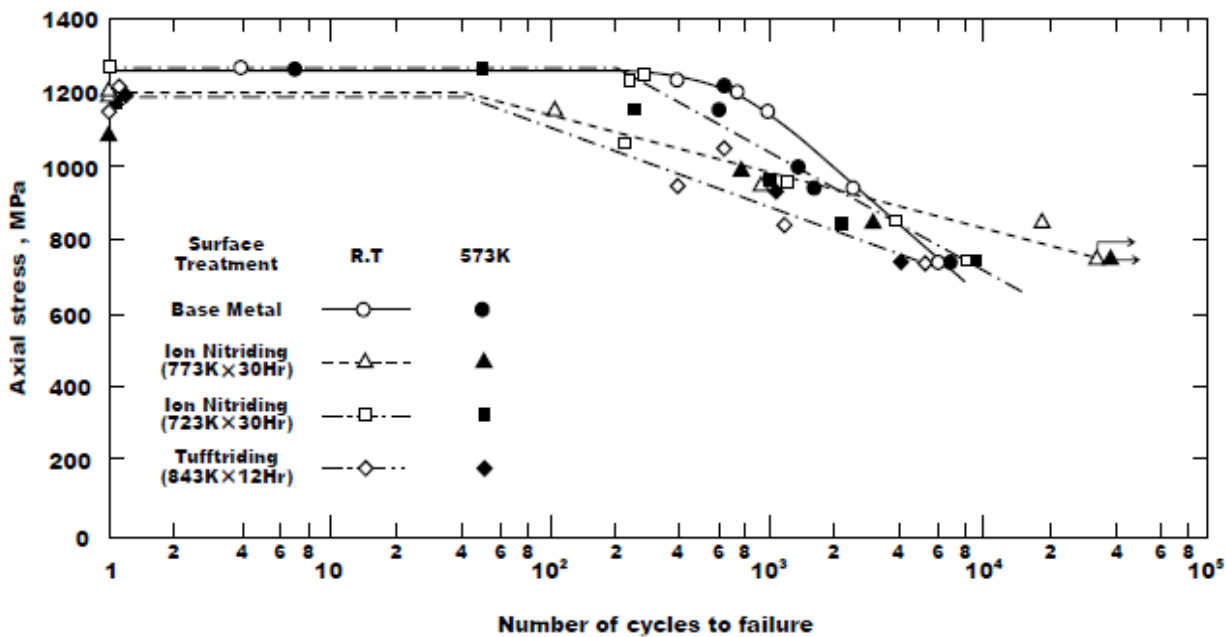


Fig. 14. Influence of surface treatments on low cycle fatigue strength of SKD62[4]

| Surface treatment | $\sigma_c/\sigma_B$ | $N_c$ ,cycles |
|---|---|---|
| Ionnitride(773Kx30h) | 0.79 | $3x10^3$ |
| Ion nitride(723Kx30h) | 0.73 | $5x10^3$ |
| Tufftride(823Kx12h) | 0.63 | $7x10^3$ |

$\sigma_c$ : Stress expected for surface hardening
$N_c$ : Number of cycles expected for surface hardening effect

Table 1. Surface hardening effect on low cycle fatigue strength of SKD62[4].

The strong reason of ineffective ion nitride effect at the higher stress amplitude can be explained by earlier fatigue crack initiation at brittle nitride compounds formed on the ion nitrided surface [11]. While ion nitride effect at lower stress amplitude can be expected by delayed fatigue crack initiation at ion nitride layer. The different effect of ion nitride effect on fatigue strength depend on surface hardness, hardened depth, properties of hardened layer and residual stress of ion nitride layer [12]. The surface treatment effect on fatigue strength of hot forging die steel is different in fatigue loading manner. The improvement effect could not be observed in reversed axial loading with mean stress [13].

Fig. 15 shows representative fracture surface morphology of SKD62 in low cycle fatigue range at 573K. Crack initiated from the notched surface (Fig. 15a), c)) and propagated with transgranular mode. Striation was identified at failed number of cycles over than $10^2$ (Fig. 15d)) and was predominantly observed on low cycle fatigue fracture surfaces at

RT, 473K and 723K. Dimple was observed at crack initiation area at failed number of cycles lower than 10 (Fig. 4b)) [4].
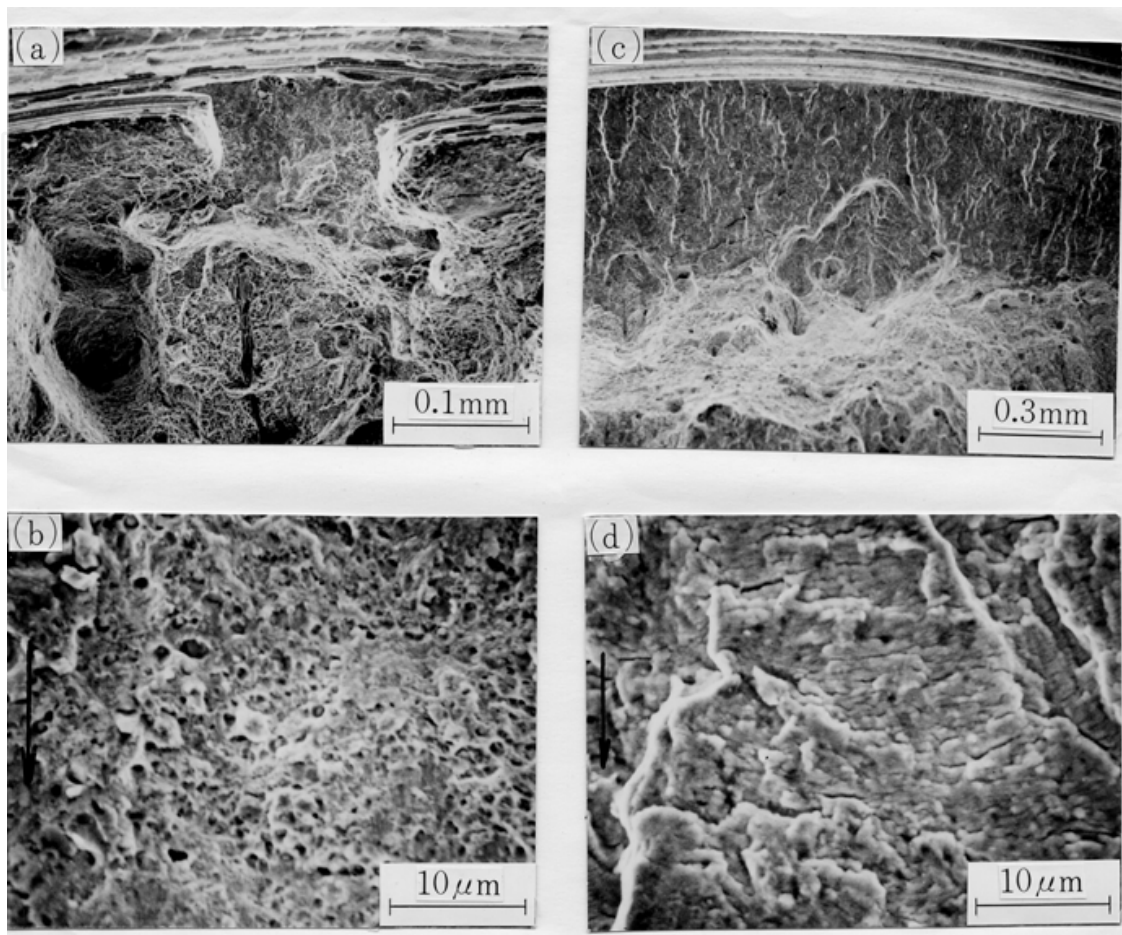


Fig. 15. Low cycle fatigue fracture surface[4]. a), b) Axial stress 1274.9 MPa, Number of cycles 7 c),d) Axial stress 1029.7 MPa, Number of cycles $1.4 \times 10^3$ b), d) are enlargement of a),c),respectively. Arrow shows crack propagation direction.

Fatigue crack propagation tests were conducted for SKD62 steels with different hardness by use of an axial fatigue testing machine (98kN). Plate specimens of 5mm thickness with a semi circular single edge notch were used. Frequency was 0.083Hz and R value was 0.05. Fig. 16 shows the crack propagation curves for SKD62 with HRC46 at [10]. The da/dN at 723K was faster than that at RT in the ΔK from 40 to 150 $MPam^{1/2}$. However, the da/dN at 473K was slower than that at RT. Further investigation on the role of oxide during crack closure may be needed to clarify this phenomenon.

Crack propagated with transgranular mode and striation was predominantly observed at crack propagation area for all tested temperatures.

Thermal fatigue tests were conducted at 473K, 673K, 873K, 1073K and 1273K by use of the laboratory made thermal fatigue testing apparatus[10]. Plate specimens of 25mm thick with an electric discharge cut of 1.52 to 4.22mm deep and 0.37 to 0.0.41 mm wide were used for thermal fatigue crack initiation test. Plate specimens with a fatigue pre-crack cut from CT specimens with 25mm thick after introducing fatigue crack were used for thermal fatigue crack propagation tests.

The number of cycles for thermal fatigue crack initiation at 673K, 873K, 1073K and 1273K was 61, 36, 22, and 1. The lower the heating temperature, the shorter the number of cycles for thermal fatigue crack initiation and thermal fatigue crack lengths were. Thermal fatigue crack initiation was not depended on the notch ratio with length to width of the specimen.
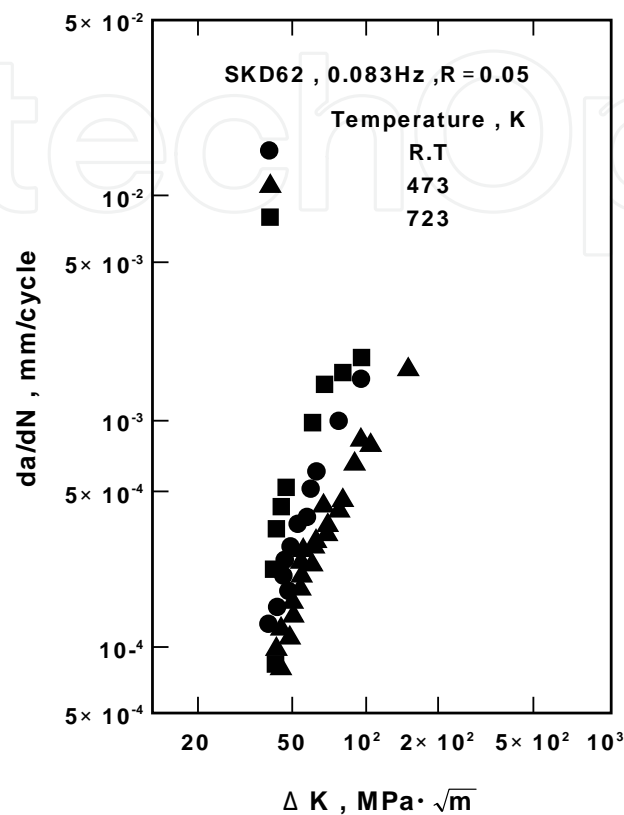


Fig. 16. Crack propagation curves of SKD62[10].

The ion nitride effect was also examined on thermal fatigue crack initiation. Thermal fatigue crack initiation was not observed up to 100 cycles at 673K. However the number of cycles for thermal fatigue crack initiation was half and the length of thermal fatigue crack was twice as compared with those of base metal at 873K. The ion nitride effect on thermal fatigue crack initiation depends on the testing temperature. Therefore in order to improve thermal fatigue life in actual hot forging dies by surface treatments the careful temperature control of hot forging dies is necessary during hot forging operation.

Thermal fatigue crack propagation tests were conducted to the number of cycles up to 100. Fig. 17 shows thermal fatigue crack propagation curves [10]. Thermal fatigue crack propagation was not observed up to 100 cycles at 473K. Thermal fatigue crack propagated up to 50 cycles, then arrested up to 100 cycles at 673K. The crack arresting phenomenon was also observed at 873K and 1073K. The cause of these phenomena is deeply related to the behavior of the oxide produced in the crack surface during thermal fatigue process. The thermal fatigue crack propagated with trangranular mode and striation like pattern were predominantly observed on thermal fatigue fracture surfaces. The typical thermal fatigue fracture surface at 873K is shown in Fig. 18. The morphology of the fracture surface and striation like pattern was very similar to the fracture surface of an actual reverse gear forging die failed after one thousand forging operations [10].
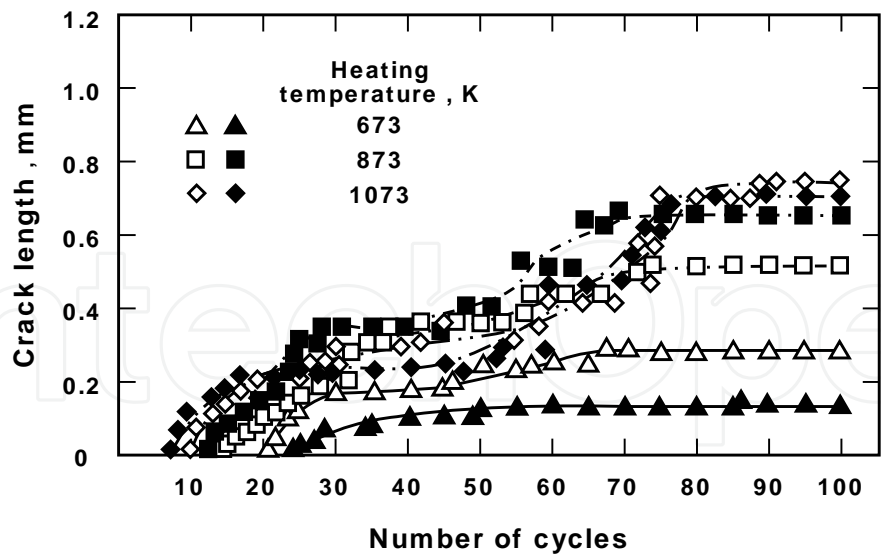
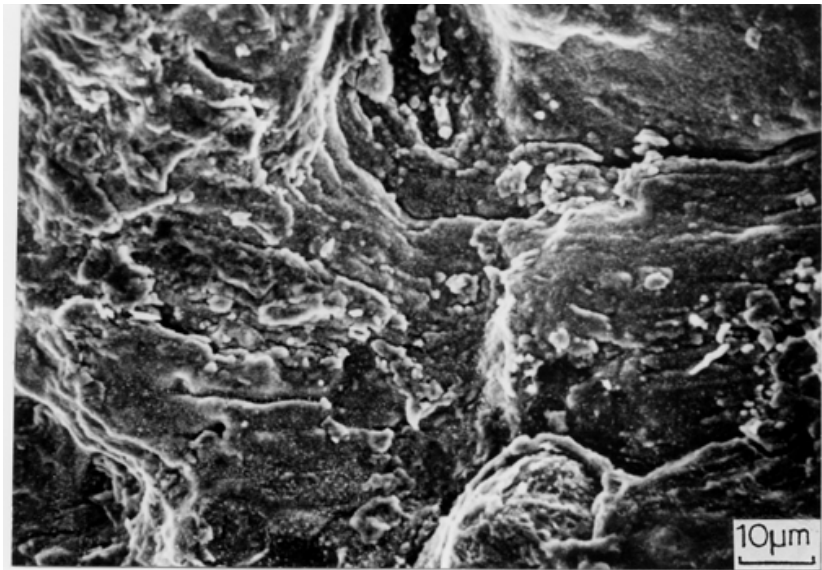Fig. 17. Thermal fatigue crack propagation curves[10].



Fig. 18. Thermal fatigue fracture surface of the specimen[10]. SKD62, Heating temperature: 873K, Number of cycles: 100

## 3.2 Cold forging die steels

Load controlled low cycle fatigue tests were conducted for representative cold forging die steels of SKH51 and YXR3 (0.65mass% C high speed steel). Ultimate tensile strength and Rockwell C scale hardness number (HRC) of SKH51 and YXR3 steel are 2550MPa,66.0 and 2240MPa,61.5,respectively. The round bar specimens with 6.5 mm at minimum diameter was used. Frequency was 20Hz and R value was 0.05.Fig.19 shows S-N curves of the lapped plane bar specimens of YXR3 and SKH51 heat-treated in vacuum [14]. Fatigue strength of SKH51 steel is higher than that of YXR3.

This is because of the higher ultimate tensile strength of SKH51 than that of YXR3 steel. Fig. 20 shows S-N diagrams of SKH51 heat treated in vacuum and salt bath. The effect of surface roughness on low cycle fatigue strength can be observed for specimen heat treated in

vacuum. However the fatigue strength of the lapped plane bar specimen was just a little lower than that in YXR3 steel [14]. The effect of surface roughness on fatigue strength is prominent at low stress amplitude in rotating bending fatigue [15]. It can be concluded that the steel with smoother surface has higher fatigue strength for SKH51 as a result of a delay in fatigue crack initiation from the surface [16].
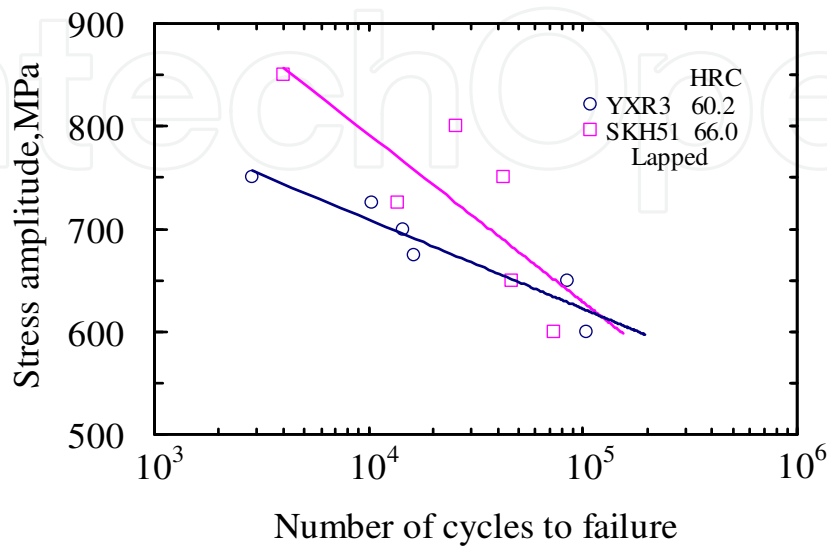


Fig. 19. S-N diagrams of the lapped plane bar specimen of SKH51 and YXR3 steel heat treated in vacuum [14].
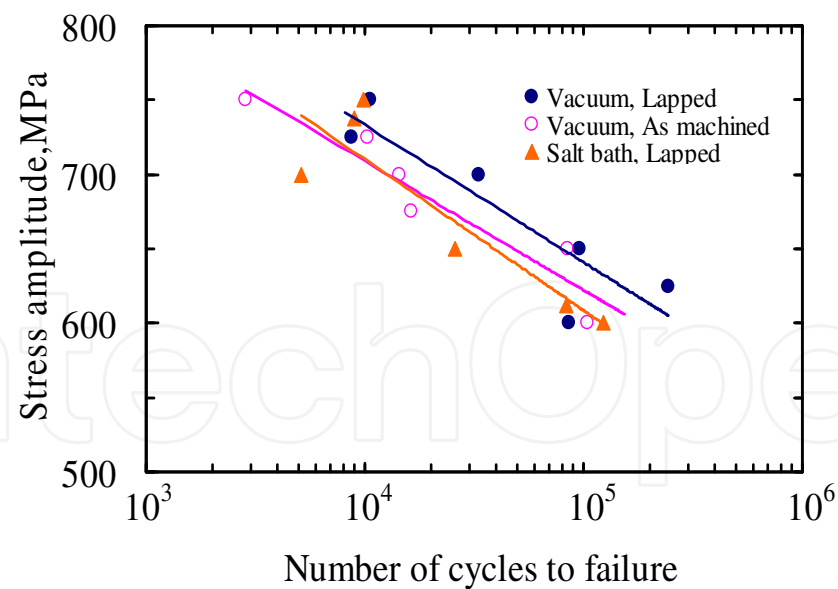


Fig. 20. S-N diagrams of SKH51 heat treated in vacuum and in salt bath[14].

Fig. 21 shows S-N diagrams of YXR notched specimens with stress concentration factor 1.5 to 2.5. Fatigue life of the notched specimen with larger stress concentration factor is shorter than that with smaller stress concentration factor. It is also apparent that fatigue life is influenced by angle of notch with same stress concentration factor. Thus low cycle fatigue strength of cold forging die steel is very sensitive to notch [14].

Ion nitride effect on fatigue strength could not be observed at number of cycles at $1.5 \times 10^4$ cycles for YXR3 steel. In YXR3 steel with higher hardness, stress expected for ion nitride effect decreased as compared with those in SKD61 steel. Higher the Vickers hardness numbers of forging die steel the lower the stress expected for ion nitride effect as observed in hot forging die steels.The strong reason of ineffctive ion nitride effect can be explained by fatigue crack initiation at brittle nitride compounds formed on the surface [17].

SEM fracture surface observation for plane bar specimens revealed that subsurface crack initiation was observed at failed number of cycles over than $8 \times 10^4$ cycles for YXR3 steel and $4.5 \times 10^4$ cycles for SKH51 steel. Transgranular fracture surfaces were predominant in crack propagation area for both steels. The typical subsurface fracture surface initiation and the transgranular fracture surface of plane bar specimen inYXR3 steel are shown in Fig. 22a) and Fig. 22b), respectively. Macroscopic fracture surface observation on notched specimens of YXR3 steel revealed that the smaller the stress concentration factor and the larger the stress amplitude the smoother fatigue fracture surface was observed [14]. Crack initiation occurred from the surface in notched specimens of cold forging die steel. Thus the crack initiation mode in notched specimens is completely different from that in plane bar specimens.
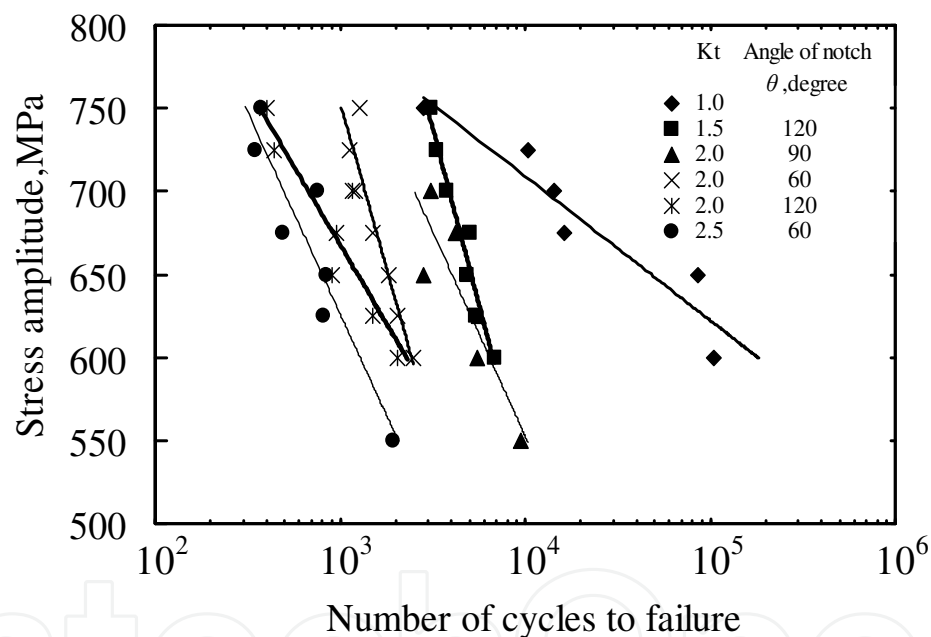


Fig. 21. S-N diagrams of YXR3 steel notched specimens with various stress concentration factor[14].

High cycle fatigue tests were conducted for quenched and tempered YXR3, 0.65 mass % carbon matrix high speed steel. Ultimate tensile strength and Rockwell C scale hardness number of this YXR3 steel was 2192MPa and 60.0, respectively. Plane bar specimen with 6.5mm at minimum diameter and notched round bar specimens with stress concentration factor with 1.5, 2.0and 2.5 were used. A hydraulic fatigue testing machine (Instron Fast track 8801, 98kN) was used. Frequency was 20Hz and R value was 0.05.

Fig. 23 shows S-N diagrams of YXR3 steel in high cycle regime [18]. In considering about the higher ultimate tensile strength of this steel, fatigue limit of 400MPa at $10^7$ cycles is low. This is because of the mean stress effect on fatigue strength of the high speed steel. The similar phenomenon was reported on low cycle fatigue strength of high speed steel, SKH51. The

low cycle fatigue data shown in Fig.21 are again plotted in Fig.23. It is apparent that the same behaviour can be observed both in low cycle and high cycle regime for plane and notched bar specimens of YXR3 steel.
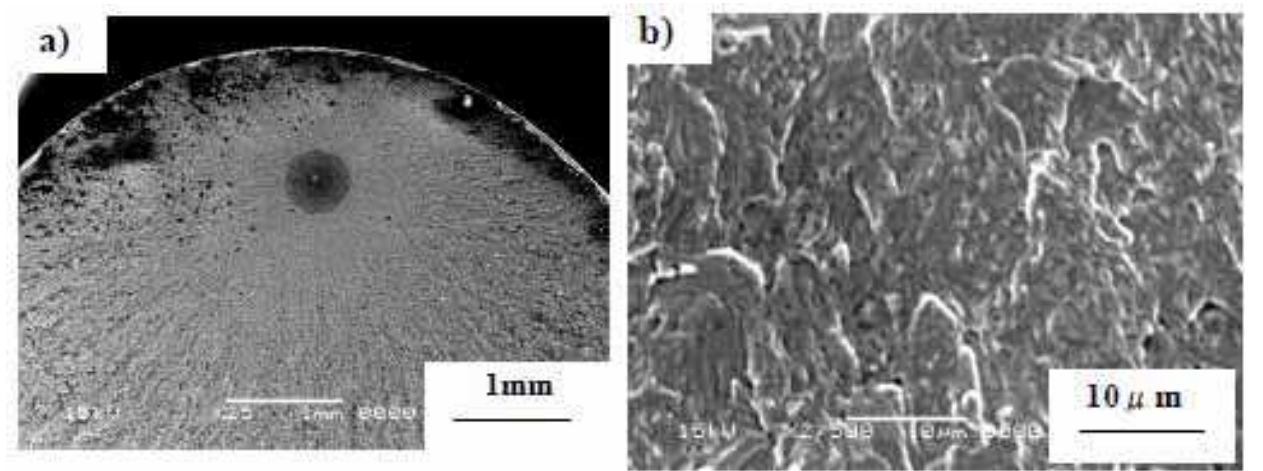


Fig. 22. Fatigue fracture surface of the lapped plane bar specimen heat treated in vacuum[14]. YXR3 steel, 600MPa, 1 x 10⁵ cycles a) initiation area  b) propagation area
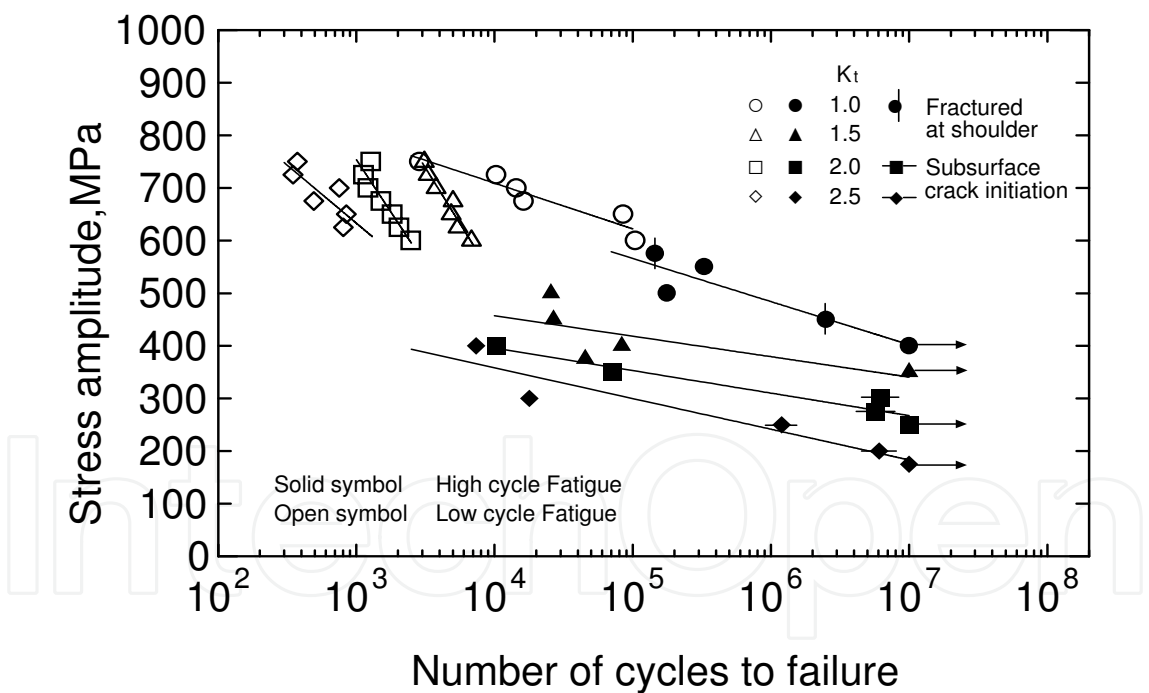


Fig. 23. S-N diagrams of notched specimens,YXR3 steel [18].

In high cycle fatigue for plane bar specimen crack initiated at subsurface as observed on low cycle fatigue fracture surfaces [18]. On the contrary crack initiation site was changed from notched surface to subsurface at failed number of cycles over than $10^6$ for all notched specimens with stress concentration factor $K_t$ of 2.0 and 2.5. Fig. 24 a),b) shows the difference of crack initiation site in notched bar specimen with stress concentration factor of 2.0. The emphasis is focused upon the change of crack initiation site in high cycle range over

than $10^6$ cycles for the notched specimen in YXR3 steel with high ultimate tensile strength of 2192 MPa. The reason of this phenomenon may be deeply related to the notch sensitivity and fracture toughness of YXR3 steel. Transgranular fracture surfaces were predominant (Fig. 24c), d)) and well defined striation were not observed in crack propagation area for all tested specimens.
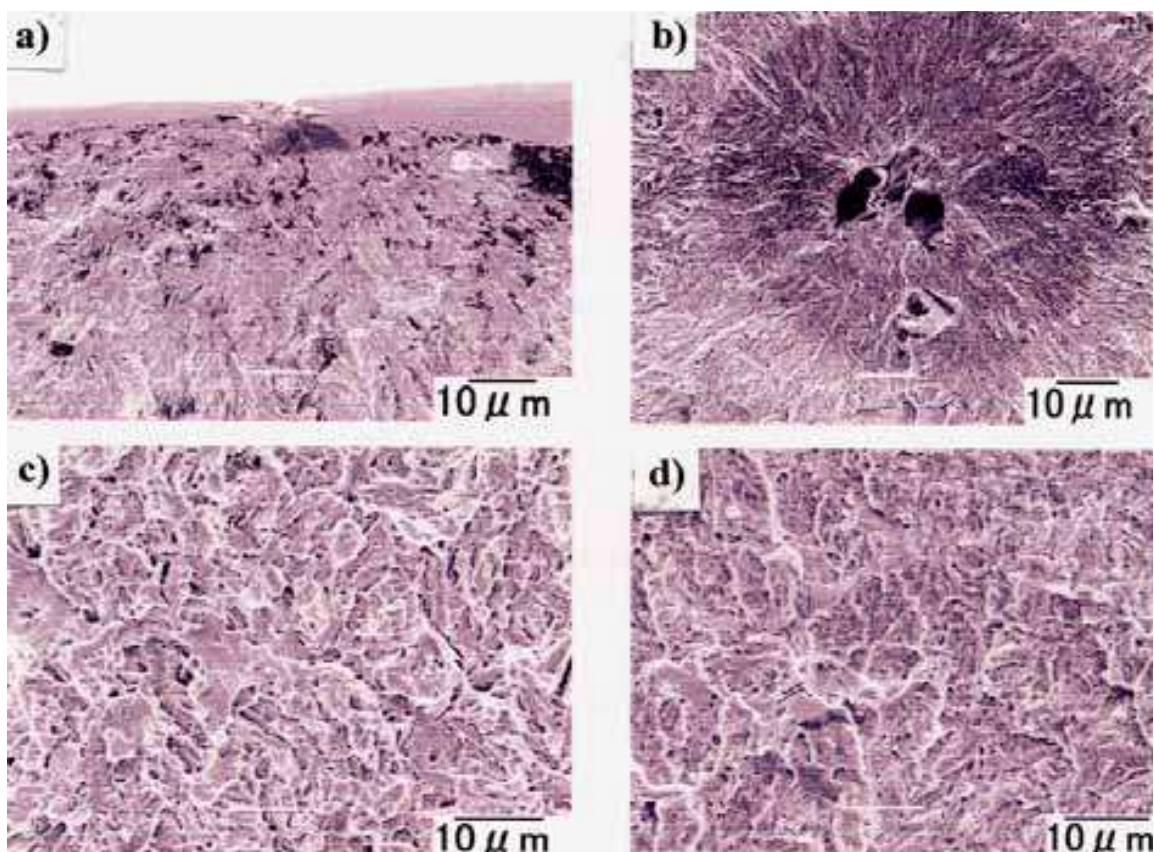


Fig. 24. Fatigue fracture surface of YXR3 steel with $K_t$=2.0[18]. a),b) crack initiation area,c)0.8mm from initiation,d)0.6mm from initiation a), c) 400MPa,1x10⁴ cycles, b), d) 300MPa,6.2x10⁶ cycles

## 4. Concluding remarks

In this chapter fatigue and fracture behavior of representative hot and cold forging die steels are summarized. However the information is still limited in materials, design, manufacturing and operations of hot and cold forging dies. In particular the fatigue crack initiation behavior of SKD62 steel is recommended to investigate. Thermal fatigue crack propagation rate is also recommended to obtain in low cycle regime. The fatigue data for other hot forging die steels except SKD62 are fundamentally needed in design of hot forging dies. For quantitative analysis of fatigue fracture surfaces of hot forging dies more information on fracture surface morphologies is absolutely needed in failure analysis. Because of the high hardness the information on fatigue strength and fatigue crack propagation is very limited on cold forging die steels. The low cycle fatigue characteristics of cold forging die steels except SKH51 and YXR3 are recommended to investigate. Fatigue crack propagation rate and fracture surface characteristics of cold forging die steels are recommended to obtain for

failure analysis of cold forging dies. In particular crack initiation mechanism for notched specimens must be clarified. Recent progress of die steel, surface treatment and stress analysis enabled to develop general failure analysis method. Besides cracking problems due to poor wear resistance must be evaluated[19]. Scientific analysis of fracture behavior of forging die steels must be usefully linked to modern technology enabled to prevent hot and cold forging die failure and to extend die life.

## 5. References

[1] R. Ebara and K. Kubota, Journal of the Japan Society for Technology of Plasticity, 23 (1982), 977-983.

[2] R. Ebara, Macro and Microscopic Approach to Faracture, S. -I. Nishida Ed. WIT Press, 2003, 243-253.

[3] R. Ebara, K. Takeda, Y. Ishibashi, A. Ogura, Y. Kondo and S. Hamaya, Engineering Failure Analysis, 16 (2009), 1968-1976.

[4] R. Ebara, K. Inoue and K. Kubota, Journal of the Soc. of Materials Science, Japan, 29(1980) 599-604.

[5] R. Ebara, K. Takeda, Y. Ishibashi, A. Ogura, Y. Kondo and S. Hamaya, Proc. of the ECF17, 2369-2376,2008.

[6] W. G. Spitzig, Trans. of the ASM,Vol.61(1961)344-348.

[7] R. C. Bates and W. G. Clark, Trans. of the ASM, Vol. 62(1969)380-388.

[8] A. J. Brothers et al.ASTM STP493,3-19,1971.

[9] R. Ebara, T. Yamane, Y. Yamamoto, H. Yajima, A. Otsuka and S. Nishimura, Mitsubishi Juko Giho(in Japanese), Vol. 17 (1980) 344-349.

[10] R. Ebara, Y. Yamada, T. Yamada and K. Kubota, Journal of Materials Science, Japan, 36(1987) 513-19.

[11] R. Ebara, International Journal of Fatigue,32(2010)830-840.

[12] H. Nakamura T, Horikawa, Fatigue strength of metal and application to fatigue strength design, 2008, Corona publishing Co.

[13] K.Fujitani S, Okazaki T, Sakai and T. Tanaka, J Soc Mater Sci. Jpn., 30 (1981) 123-127.

[14] R. Ebara, J. Katayama, S. Yamamoto, R. Ueji, K. Kawamura, A. Ogura, Y. Kondo and S. Hamaya, Fatigue and Plasticity: From Mechanisms to Design, Proc. of the 12 th International Spring Meeting; 257-264, 2008, SF2M.

[15] M. Shinohara et al., J. Japan Soc for Tech of Plasticity, 22(1981).159-165.

[16] H. Kobayash, R. Ebara, A. Ogura, Y. Kondo and S. Hamaya, Proc. of the fourth Intern. Conf. on Very High Cycle Fatigue, Allison J. E., J. Jones W, Larsen J. M. and R.O.Ritchie R O, Ed., 319-324, 2007, TMS.

[17] T. Yamashita, T. Bito, R. Ebara and K.Kubota, Proc. of the International Conference on Advanced Technology in Experimental Mechanics, 2007, CDROM, JSME.

[18] R. Ebara, R. Nohara, R. Ueji, A. Ogura Y. Ishihara and S. Hamaya, Key Engineering Materials, 417-418(2010)225-228.

[19] R. Ebara and K. Kubota, Engineering Failure Analysis, 15 (2008)881-893.
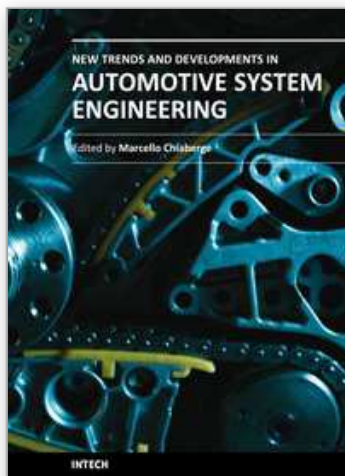
**New Trends and Developments in Automotive System Engineering**

Edited by Prof. Marcello Chiaberge

In the last few years the automobile design process is required to become more responsible and responsibly related to environmental needs. Basing the automotive design not only on the appearance, the visual appearance of the vehicle needs to be thought together and deeply integrated with the â€œpowerâ€ developed by the engine. The purpose of this book is to try to present the new technologies development scenario, and not to give any indication about the direction that should be given to the research in this complex and multi-disciplinary challenging field.

**How to reference**

In order to correctly reference this scholarly work, feel free to copy and paste the following:

Ryuichiro Ebara (2011). Fatigue and Fracture Behavior of Forging Die Steels, New Trends and Developments in Automotive System Engineering, Prof. Marcello Chiaberge (Ed.), ISBN: 978-953-307-517-4, InTech, Available from: http://www.intechopen.com/books/new-trends-and-developments-in-automotive-system-engineering/fatigue-and-fracture-behavior-of-forging-die-steels

# INTECH
open science | open minds